

# Space-time nature of causality

Ezequiel Bianco–Martinez<sup>1</sup> and Murilo S. Baptista<sup>2, a)</sup>

<sup>1)</sup>*IBM Analytics, IBM, Amsterdam*

*Institute of Complex Sciences and Mathematical Biology, University of Aberdeen, SUPA, Aberdeen, UK*

<sup>2)</sup>*Institute of Complex Sciences and Mathematical Biology, University of Aberdeen, SUPA, Aberdeen, UK*

(Dated: 3 September 2022)

In a causal world the direction of the time arrow dictates how past causal events in a variable  $X$  produce future effects in  $Y$ .  $X$  is said to cause an effect in  $Y$ , if the predictability (uncertainty) about the future states of  $Y$  increases (decreases) as its own past and the past of  $X$  are taken into consideration. Causality is thus intrinsic dependent on the observation of the past events of both variables involved, to the prediction (or uncertainty reduction) of future event of the other variable. We will show that this notion of causality leads to another natural definition for it: to detect whether a system  $X$  causes an effect in system  $Y$ , observations of past and future events in only the variable  $Y$  is sufficient to predict past states of  $X$ , or to reduce the uncertainty about the past state of  $X$ . This fundamental time property of causality will lead to a fundamental spatial property of causality. To detect a flow of influence from  $X$  to  $Y$ , either one can measure the symmetric quantity mutual information between shorter time-series of  $X$  and longer time-series of  $Y$ , an approach that explores the time nature of causality, or one can calculate the mutual information between lower precision measured time-series in  $X$  and higher precision measured time-series in  $Y$ , an approach that explores the space nature of causality. Causality has thus space and time signatures, causing a break of symmetry in the topology of the probabilistic space, or causing a break of symmetry in the length of the measured time-series, a consequence of the fact that information flows from  $X$  to  $Y$ .

## INTRODUCTION

In a causal world the direction of the time arrow dictates how past causal events produce future effects. The determination of the direction and the intensity of the arrow of influence, causality, is one of the first questions one tries to answer in order to model a system. In ecology, it is fundamental to understand whether zooplankton concentration drives fish population. In meteorology, one wishes to determine whether and how surface sea temperature affects atmospheric temperature in different parts of the globe, or how green house gases drive global temperature. In finance, tax and expenditure correlates with saving and growth. In geology, one wants to access the direction of the flows of underground water from some measurements of water reservoir levels. In urbanism, one wants to understand how electricity consumption drives (or is driven by) urbanism or how building environment leads to obesity. Given the relevance of the topic, several methods have been developed in the last decades to study causality. Among them, there are the approaches that access causality based on informational quantities. They are sustained by the fundamental idea if  $X$  causes an effect in  $Y$ , then uncertainty about future states of  $Y$  is reduced by considering the past of  $Y$  and the past of  $X$ ,

a hypothesis that implicitly adopts the Granger causal idea that observations in the past of both  $X$  (causing system) and  $Y$  (where the effect is produced) can be used to predict the future state of  $Y$ . This work aims at unifying the Granger definition of causality defined in terms of predictability with those based on information quantities by studying the dynamical fundamental of causality. We will show that a system  $X$  causes an effect in a system  $Y$ , if *solely* observations in  $Y$  can be used to predict the past states of the system  $X$ , an observation that will lead us to propose a new informational theoretic quantity to determine the direction of causal events that we name Causal Mutual Information. Along the way to demonstrate this fundamental intrinsic dynamical property of causality, we will show that causality has space and time signatures, and each signature can be advantageously explored to study the direction of influence in different systems. Moreover, we will show that our quantity allows for a simple and less computational demanding approach, but rigorous, quantification of causality.

The determination that a past event in a system has caused a present effect on another system provides a straight measurement of the direction of influence in these systems. Causal relationships between two events happening in two different systems  $X$  and  $Y$  can be established by verifying whether past events in  $X$  and  $Y$  influence future events in  $Y$ . Such understanding is fundamental to characterise, model, and predict behaviour in natural, social, and technological systems. The study of the cause-effect relationships is defined as causality.

<sup>a)</sup>murilo.baptista@abdn.ac.uk

Causality is a concept that involves the temporal relationship among past, present and future events of variables. Our studies show however that the temporal nature of causality from  $X$  to  $Y$  can not only be redefined in terms of the reduction of uncertainty from the variable  $X$  solely based on observations in the past, present and future, of  $Y$ , but also that causality can be defined in terms of the topological feature of the probabilistic space. In a deterministic system, two temporally related events defined by two particular states of the system are also intrinsically related in space. This space-time ergodic duality in a deterministic system indicates that time-causality should lead to space-causality, a property that we will explore in this work to create novel ways to quantify causality.

When a perturbation affects a system, its influence is transmitted from the perturbation's source to the other variables of the system. The path the perturbation takes to propagate within the system can be predicted analysing the causality of events in the system. A smart way to study causality is through a controlled experiment where perturbations can be designed to extract the causal structure of the system. However, the desired experiment could be too expensive, technically impossible to perform, or too invasive. Therefore, it is important to develop methods to identify the causal structure of a system only from observational data, without employing any perturbative technique. The identification of the causing and affected systems from observational data has been of great interest for many scientists. Consequently, and also because the identification of causality is fundamental to the effective observation, modelling, and controlling of any complex system, several techniques to infer and quantify causality have been recently proposed<sup>1-11</sup>.

Granger<sup>4,12,13</sup> considered that if a variable  $x(t)$  causes an effect in  $y(t)$ , then predictions of  $y(t)$  are improved by considering its own past complemented by the past of  $x(t)$ . Based on this assumption, he constructed statistical tests to validate this hypothesis. To adopt this hypothesis to study causality from data by constructing linear models, Granger causality introduce measures mostly used in correlation based approaches (directed partial coherence)<sup>14</sup>, Directed Coherence<sup>15</sup>, Partial Direct Coherence<sup>16</sup>, direct Directed Transfer Function<sup>17</sup>, which are capable of identifying interactions in linear systems, but are not suitable to detect causality among subsystems composing a non-linear system<sup>8</sup>. Due to this, methods based on Granger causality appropriated to detect causality in nonlinear system were developed<sup>9,10</sup>. Granger causality can also be adopted by informational theoretical quantities, of special interest to us, such as the Transfer Entropy<sup>5</sup>, Directed Information Theory<sup>14,18</sup>, Conditional Mutual Information<sup>6</sup>, Partial Transfer Entropy<sup>19</sup>, and Mutual Information from Mixed Embeddings (MIME)<sup>20</sup>, which explore the intuitive notion that if system  $X$  causes an effect in system  $Y$  then, as specifically defined by transfer entropy, the amount of uncertainty in future values of  $Y$  is reduced by knowing

the past values of  $X$  given past values of  $Y$ .

In this work, along the lines of the work in Ref.<sup>14</sup>, we intend to unify the concept of causality based on predictability introduced by Granger with the concept of causality defined in terms of transfer entropy, using for that a new unnoticed informational quantity that fully explores the space-time properties of causality, and that we call Causal Mutual Information (CaMI).  $\text{CaMI}_{X \rightarrow Y}$  measures the total amount of information being transmitted from  $X$  to  $Y$ , including both the information shared between both variables and that can be used to predict the present state of  $X$  by observations in  $Y$ , and the information causally transmitted from  $X$  to  $Y$  and that can be used to predict the past states of  $X$  by observations of the past and future states of  $Y$ . To highlight the space-time properties of causality, we mostly study coupled deterministic systems, but assume that measurements cannot obtain the precise location of the state of a variable, but the error is bounded, so, we assume that there is bounded observational noise.

Our proposed definition of causality, quantified by the quantity CaMI, is based on the physical notion that if  $X$  causes effect in  $Y$ , then longer observations of the variable  $Y$  (or alternatively higher resolution observations) than the one considered for  $X$  can be used to predict the past of  $X$ . CaMI is calculated only by the probabilities of joint events, without the need of conditional events. This allows one to do a reduction in the dimensionality of the probability space used to quantify causality, resulting in a method that demands low computational power, and therefore allows for a quick assessment of causality. Then, we show that the topology of the probabilistic space determined by the shapes and forms of the partitions being generated by a dynamical process can also be used to quantify causality. As a consequence, it is possible to state the direction of causality only by inspecting the topology of points in the probabilistic space defined by the measured variables. A practical use of the topological features of these probabilistic spaces is the determination of localised regions, the causal bubbles, that define ranges for the variables that are responsible for most of the information transmitted between two systems, and that can be used to demonstrate that if there is a flow of information from the variable  $X$  to  $Y$ , then it is also true that observations in  $Y$  allows for the prediction of location of the past states of variable  $X$ . As we shall see, there are preferential places and preferential times to measure the information being transmitted.

An advantage of our approach is that even though the analysis of causality is bivariate, employing two observables taken from two subsystems  $X$  and  $Y$  in a larger system, the topological properties of the constructed probabilistic space can discern whether information is being sent physically from  $X$  to  $Y$ , or whether it is being mediated by other subsystems and variables (in this case, there is no physical connection between  $X$  and  $Y$ ). This special property of the probabilistic space to detect causality allows one to detect direct or mediate effects

without the need to calculate multivariate conditional probabilities, from which one can detect direct or mediated influences in stochastic systems Ref.<sup>11,21</sup>, an approach suitable for both dynamical and stochastic systems, but that however requires the use of large dimensional probabilistic spaces. In the multivariate approach to detect causality, the conditional probabilities of multivariate variables need to take into consideration the influence of co-founders<sup>22</sup>, entities that mediates the transfer of information from  $X$  and  $Y$  systems.

## I. COUPLED MAPS

For this study of causality, we consider discrete coupled maps, whose connected nodes are described by:

$$x_{n+1}^i = f(x_n^i, r)(1 - \alpha) + \frac{\alpha}{k_i} \sum_{j=1}^M A_{ij} f(x_n^j, r), \quad (1)$$

where  $x_n^i$  is the trajectory of map  $i$ ,  $n$  is the time index of the variable of the dynamics,  $\alpha \in [0, 1]$  is the coupling parameter,  $A_{ij}$  is the adjacency matrix (with entries of 1 or 0 depending on the existence of a connection between two nodes or not, respectively),  $r$  is the fixed parameter of each map,  $k_i$  is the degree of node  $i$  ( $k_i = \sum(A_{ij})$ ) and  $f(x_n, r)$  is the map governing the dynamics that can be described by the Logistic map  $f_1(x_n, r) = rx_n(1 - x_n)$ <sup>23</sup>. A disconnected node ( $k_i = 0$ ) is described by  $x_{n+1}^i = f(x_n^i, r)$ . We assume there are  $N_d$  maps forming the network.

Giving two variables  $X$  and  $Y$ , we are interested in determining the direction of influence that one variable imposes over the other one. If  $X$  influences  $Y$ , we represent this interaction by  $X \rightarrow Y$ .

## II. PARTITIONS, STATE AND PROBABILISTIC SPACE, AND SYMBOLIC TRAJECTORIES

In what follows, we consider that marginal observations are being made in the relevant variables, defining events in one variable by the falling of a trajectory point within an interval. This interval represents the resolution of the observer. These marginal observations and their probabilities, will be used to calculate the probabilities to quantify causality. For simplicity in our analysis, we encode these partitions into symbols, and treat the trajectories as symbolic trajectories.

### A. Order- $m$ Partitions, symbolic representation, and dynamics on it

Consider two discrete scalar time-series  $\mathbf{X} = \{x_0, x_1, x_2, \dots, x_{n-1}\}$  and  $\mathbf{Y} = \{y_0, y_1, y_2, \dots, y_{n-1}\}$  with  $n$  elements, and  $\Phi = \{\mathbf{X}, \mathbf{Y}\}$  defines a pair of variables taken from two subsystem in a complex network or

coupled system. Therefore, a point in a 2-dimensional state space  $\Omega^{XY}$  with coordinates  $[\mathbf{X} \times \mathbf{Y}]$  representing the states of the subsystems  $\Phi$  at time  $t$  has coordinates  $\{x_t, y_t\}$ .

We define a marginal partition of order- $m$  of the coordinate  $X$  as  $\mathcal{C}^X(m)$ , defined by the boundary curves  $\mathcal{L}_X(m) = \{l_1^X(m), \dots, l_r^X(m)\}$ , which in this thesis are assumed to be straight lines, orthogonal to the direction of  $X$ . Then, this partition is composed by columns  $\mathbf{c}_i^X(m)$  where each one is separated from any other by one and only one curve  $l_i^X(m) \in \mathcal{L}_X(m)$ . Similarly, for the coordinate  $Y$  we can define a marginal partition  $\mathcal{C}^Y(m)$ , formed by rows  $\mathbf{c}_i^Y(m)$ , enclosed by the set of boundary curves  $\mathcal{L}_Y(m) = \{l_1^Y(m), \dots, l_r^Y(m)\}$ , which are in this work assumed to be straight lines, orthogonal to the direction of  $Y$ . Since we have a 2D time-series, we can construct a space partition  $\mathcal{C}^{XY}(m)$  as a splitting of the space  $\Omega^{XY}$  formed by the union of the lines in  $\mathcal{L}_X(m)$  and  $\mathcal{L}_Y(m)$ , so

$$\mathcal{C}^{XY}(m) = \mathcal{C}(m)^X \cup \mathcal{C}(m)^Y. \quad (2)$$

Areas enclosed by the straight lines of  $\mathcal{C}^{XY}(m)$  form the cells  $\mathbf{c}_i^{XY}(m)$  of the partition  $\mathcal{C}^{XY}(m)$  that are encoded by the symbols  $\mathfrak{s}_i^{XY}(m)$ .  $S^{XY}(m)$  represents all the possible symbols encoding cells in the partition of order- $m$ .

The dynamics of point in this partition is represented by the transformation  $\mathcal{U}_t: (x_{i+1}, y_{i+1}) = \mathcal{U}_t(x_i, y_i)$ , and  $\mathcal{U}_t^p(x_t, y_t) = (x_{t+p}, y_{t+p})$ . The symbolic dynamics of points in this partition is regulated by the transformation  $\mathcal{T}$ , a surjective mapping of the states of variables in  $\Omega^{XY}$  to a specific symbol in  $S^{XY}(m)$ .  $\mathcal{T}$  provides a symbolic sequence  $\Phi$  in the partition  $\mathcal{C}^{XY}(m)$ . From Eq. (1),  $\mathcal{T}$  is the transformation that maps points from  $\Omega^{XY}$  into itself, a 2D projection of the whole  $N_d$ -dimensional network.

Given the partition  $\mathcal{C}^{XY}(m)$ , we define a transition matrix  $\Pi(m)$  where the element  $\Pi(m)_{ij} = 1$  if the cell  $\mathbf{c}_i^{XY}(m)$  is the pre-image of the cell  $\mathbf{c}_j^{XY}(m)$  (i.e., there is a dynamical evolution from cell  $\mathbf{c}_i^{XY}$  to cell  $\mathbf{c}_j^{XY}$ ).

We define a *transition matrix of order- $m$*  ( $\Pi_{\Phi}(m)$ ) as:

$$\Pi_{\Phi_{ij}}(m) = \begin{cases} 1 & \text{if } F^m(\mathbf{c}_i) \cap \mathbf{c}_j \neq \emptyset \\ 0 & \text{Otherwise} \end{cases} \quad (3)$$

A partition is defined as an order- $m$  if it generates a transition matrix of order  $m$ .

We adopt a partition defined by marginal probabilities because we want to define informational measures that quantify the predictability one has to predict the state of one variable by measuring only the state of the other variable.

### B. Probabilistic space and symbolic trajectory

Now, let us define a  $L$  time-delay and time-forward coordinate system from which probabilities are calculated.

The time-delay trajectory  $\Phi_{-L}(t) = \{X_{-L}(t), Y_{-L}(t)\} = \{x_{t-L}, \dots, x_{t-1}, y_{t-L}, \dots, y_{t-1}\}$  represents a short segment with length  $L$  (e.g.  $L$  points) of the time-series  $\Phi(t)$  taken for a time span between the integer time  $t - L$  until the time  $t - 1$ , the time  $t$  representing the time moment from where past and future are defined. By applying the transformation  $\mathcal{T}$  to a segment of length  $L$  of the time-series  $\Phi_{-L}(t)$ , we generate a sequence of symbols that represent the itinerary followed by the past length- $L$  trajectory. The trajectory points  $\Phi_{-L}^\sigma(t)$  follow an itinerary along the partitions  $\mathcal{C}^X(m)$  ( $\sigma \equiv X$ ),  $\mathcal{C}^Y(m)$  ( $\sigma \equiv Y$ ), or  $\mathcal{C}^{XY}(m)$  ( $\sigma \equiv XY$ ), which are given by  $\{c_{i_{t-L}}^\sigma(m), c_{i_{t-L+1}}^\sigma(m), \dots, c_{i_{t-1}}^\sigma(m)\}$ . If  $\sigma = XY$ , then  $(x_{t-L}, y_{t-L}) \in c_{i_{t-L}}^{XY}(m)$ . If  $\sigma = X$ , then  $x_{t-L} \in c_{i_{t-L}}^X(m)$ . The itinerary  $\mathcal{C}_{-L}^\sigma(t, m) = \{c_{i_{t-L}}^\sigma(m), c_{i_{t-L+1}}^\sigma(m), \dots, c_{i_{t-1}}^\sigma(m)\}$  is encoded by a symbolic sequence  $S_{-L}^\sigma(t, m) = \{s_{i_{t-L}}^\sigma(m), s_{i_{t-L+1}}^\sigma(m), \dots, s_{i_{t-1}}^\sigma(m)\}$ , from which probabilities can be calculated. Similarly, the forward-time trajectory  $\Phi_L^\sigma(t) = \{X_L(t), Y_L(t)\}$  follows an itinerary (or visits the sequence of cells)  $\mathcal{C}_L^\sigma(t, m) = \{c_{i_{t+1}}^\sigma(m), c_{i_{t+2}}^\sigma(m), \dots, c_{i_{t+L-1}}^\sigma(m)\}$  that is encoded by the symbolic sequence  $S_L^\sigma(t, m) = \{s_{i_{t+1}}^\sigma(m), s_{i_{t+2}}^\sigma(m), \dots, s_{i_{t+L-1}}^\sigma(m)\}$ .

An  $(k + m)$ -order partition  $\mathcal{C}^\sigma(k + m)$  is generated by the  $k$ -pre-iteration of the boundary curves composing the  $m$ -order partition  $\mathcal{C}^\sigma(m)$ . The pre-iteration is given by the evolution operator  $\mathcal{U}^{-k}$ . This order- $(k + m)$  partition is formed by the cells  $c_i^\sigma(k + m)$ . Notice that a cell  $c_i^{XY}(k + m) \in \mathcal{C}^{XY}(m + k)$ , with  $\mathcal{C}^{XY}(m + k) \equiv \mathcal{U}^{-k}(\mathcal{C}^{XY}(m))$  in an order- $(k + m)$  partition represents points that follow a particular length- $L = k + m$  symbolic itinerary (or length- $L$  trajectory) in the order-1 partition. The probability measure of a length- $L$  itinerary  $\mu(\{c_{i_{t-L}}^\sigma(1), c_{i_{t-L+1}}^\sigma(1), \dots, c_{i_{t-1}}^\sigma(1)\})$  is assumed to be equal to the probability measure of points in a cell of an order- $L$  partition and given by  $\mu(\{c_i^\sigma(L)\})$ , with  $x_{t-L} \in c_i^\sigma(L)$ . Many length- $L$  trajectories can follow the same itinerary. We also have that the probability  $P$  calculated over the symbolic sequence of a length- $L$  itinerary  $P(\{s_{i_{t-L}}^\sigma(1), s_{i_{t-L+1}}^\sigma(1), \dots, s_{i_{t-1}}^\sigma(1)\})$  along the order- $m$  partition. If the partition is generating, then this probability is also equal to the probability of points to belong to a cell  $s_i(L)$  of an order  $L$  partition and given by  $P(s_i(L))$ , with  $i$  such that  $\mathcal{T}(X_{-L}) = s_i(L)$ , where  $s_i(L)$  is a length- $L$  symbolic sequence that gives the name of a cell in an order- $L$  partition.

Thus, there are two ways of calculating probabilities. One based on the probability of the trajectory itineraries, which produce the probability measures  $\mu$  and the other based on the symbolic itinerary, which produces the probability measures  $P$ . There is however a fundamental difference between both probabilities. Whereas  $\mu$  is calculated over a higher  $(m + k)$ -order partition with non-overlapping well defined cells, and therefore, it requires the use of a generating partition,  $P$  refers to the probability of a symbolic sequence defined by the marginal

lower  $m$ -order original partition. It therefore does not require that the higher-order partition is generating. In our practical numerical calculations, we adopt the probabilities  $P$  to calculate our informational quantities.

For the following analytical arguments and illustration, we assume however that the higher-order partitions are generating. We also assume in the following that the initial partition is order-1 ( $m = 1$ ), therefore, there is only one straight line in  $\mathcal{L}_X(1)$  and one straight line in  $\mathcal{L}_Y(1)$ . Each of these symbolic itineraries along the order-1 original partition can be encoded by the symbolic name of a cell in an order- $L$  partition. An event in  $\mathcal{C}^{XY}(1)$  is defined by trajectory points falling in  $c_i^{XY}(1) \in \mathcal{C}^{XY}(1)$ .

### C. A generating partition

An order- $m + k$  partition  $\mathcal{C}^\sigma(m + k)$  is generated from an order- $m$   $\mathcal{C}^\sigma(m)$  by

$$\mathcal{C}^\sigma(m + k) = \mathcal{U}^{-k}(\mathcal{C}^\sigma(m)). \quad (4)$$

The partition  $\mathcal{C}^\sigma(m)$  is a "generating" partition if the all the cells in  $\mathcal{C}^\sigma(m + k)$  are non-overlapping and the union of the partition boundary curves in an order- $(m+1)$  partition restores the boundary curves of an order- $(m)$  partition.

### D. An example

As an example of how trajectory points visit the partition with different orders and how this trajectory is symbolic encoded and probabilities are calculated, we consider a dynamic process along a 1D binary partition. Assume  $x_t \in \mathcal{C}^X(1)$ . Then,  $\Phi_{-L}^X(t) = \{x_{t-L}, x_{t-L+1}, \dots, x_{t-1}\} = X_{-L}(t)$  and  $\Phi_L^X(t) = \{x_t, x_{t+1}, \dots, x_{t+L-1}\} = X_L(t)$ , and  $S_{-L}^X(t, 1) = \{s_{i_{t-L}}^X(1), s_{i_{t-L+1}}^X(1), \dots, s_{i_{t-1}}^X(1)\}$  and  $S_L^X(t, 1) = \{s_{i_t}^X(1), s_{i_{t+1}}^X(1), \dots, s_{i_{t+L-1}}^X(1)\}$ . Observing a trajectory composed by  $\{X_{-L}(t), X_L(t)\}$  considering the partition  $\mathcal{C}^X(1)$  allow us to conclude that the trajectory of the system has visited a sequence of cells described by a sequence of symbols  $\{S_{-L}^X(t, 1), S_L^X(t, 1)\}$ .

Assuming  $L = 2$ , it exists an order-2 partition generated by  $\mathcal{U}^{-1}(\mathcal{C}^X(1))$  whose cells represent intervals where points within generate  $S_{-2}^X(t, 1)$  and  $S_2^X(t, 1)$ . Moreover, a cell in an order-2 partition is encoded by a symbol that represents the whole symbolic sequence of length-2 trajectories along the partition  $\mathcal{C}^X(1)$ , and therefore there exist  $i$  such that  $s_i^X(2) = S_{-2}(t, 1)^X$  and there exist  $j$  such that  $s_j^X(2) = S_2(t, 1)^X$ . Consequently,  $P(s_i^X(2)) = P(S_{-2}(t, 1)^X)$  and  $P(s_j^X(2)) = P(S_2(t, 1)^X)$ .

In Fig. 1, we can see the relationship between a trajectory of length-4 in an order-1 and an order-2 partitions. This figure also illustrates how an order-2 partition is generated from an order-1 partition.

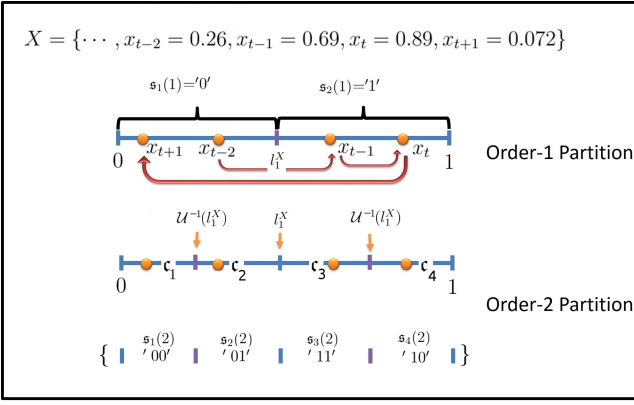


FIG. 1. In this diagram a length-4 trajectory is plotted in the state space and two partitions are shown, one of order-1 defined by the line  $l_1^X$  (and the borders of the state space) and another of order-2 defined by the union of  $l_1^X$  with  $U^{-1}(l_1^X)$ . The trajectory along the order-1 partition generates the symbolic itinerary  $\{S_{-L}^X(1), S_L^X(1)\} = \{s_{t-2} = '0', s_{t-1} = '1', s_t = '1', s_{t+1} = '0'\}$  and along the order-2 partition generates the symbolic itinerary  $\{S_{-L}^X(t, 2), S_L^X(t, 2)\} = \{s_{t-2}(2) = '01', s_{t-1}(2) = '11', s_t(2) = '10', s_{t+1}(2) = '00'\}$ . Notice, however, that the first symbol in  $s_t(2) = '10'$  represents the present location in an order-1 partition and the second symbol represents the location of the first iteration. Therefore, the second symbol in  $s_t(2) = '10'$ , represents the same first symbol in  $s_{t+1}(2) = '00'$

### E. Probabilistic spaces and informational quantities

We now define some notations for the probabilities and informational quantities to simplify the exposition of our next derivations.

The notations  $P(X_L)$  or  $P(Y_L)$  represent  $P(c_i^{X_L}(L))$  or  $P(c_i^{Y_L}(L))$ . So,  $P(X_L)$  represents the probabilities of finding points in the cells  $c_i^{X_L}(L)$  or similarly  $P(X_L) = P(s_i^{X_L}(L))$ . Therefore, the Shannon's entropy of length- $L$  symbolic sequences, represented by  $H(X_L)$  or  $H(X_{-L})$ , is calculated by

$$H(X_L) = - \sum_i P(c_i^{X_L}(L)) \log(P(c_i^{X_L}(L))), \quad (5)$$

So, if the "generating" property of the partition holds, entropies of length- $L$  trajectories along an order-1 partition space can be calculated by the measure of the cells in the higher-order partitions considered. This approach is specially oriented for analytical derivations based on the study of networks of coupled dynamical systems. Otherwise, in an experimental situation or when dealing with time-series coming from experiments or numerical simulations, one should calculate entropies considering the probabilities of different symbolic sequences observed along the order-1 partition. So,

$$H(X_L) = - \sum_i P(s_i^{X_L}(L)) \log(P(s_i^{X_L}(L))), \quad (6)$$

where  $s_i^{X_L}(L)$  represents a length- $L$  symbolic sequence, or if the partition is generating, the symbolic sequence that gives the name of a cell in an order- $L$  partition.

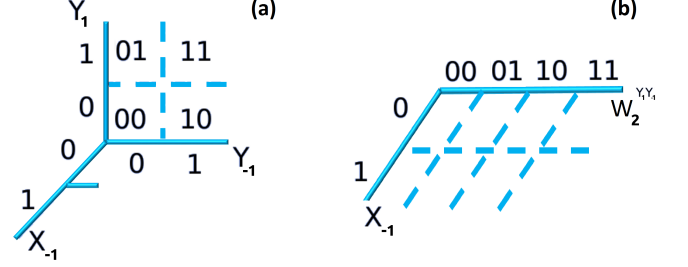


FIG. 2. (a) Visualization of the space  $\Omega^{X_{-L}Y_{-L}Y_L}$  formed by the coordinates  $(X_{-1}, Y_{-1}, Y_1)$  and an order-1 partition in each subspace formed by pair of coordinates. (b) Visualization of the reduced-dimensional space with coordinates  $(X_{-1}, W_2^{Y_{-1}Y_1})$  and its asymmetric partition. Along  $X_{-1}$  an order-1 partition is considered. Along  $W_2^{Y_{-1}Y_1}$  an order-2 partition is considered.

Let us now define a 2-dimensional state space  $\Omega^{X_{-L}Y_{-L}} \equiv [X_{-L} \times Y_{-L}]$  and with a trajectory  $\Phi^{X_{-L}Y_{-L}}$  on it.

The joint entropy of a composed space  $H(X_L, Y_L)$  is then defined by

$$H(X_L, Y_L) = - \sum P(c_i^{X_L Y_L}(L)) \log(P(c_i^{X_L Y_L}(L))). \quad (7)$$

If the generating property of the partitions does not hold, then

$$H(X_L, Y_L) = - \sum_i P(s_i^{X_L Y_L}(L)) \log(P(s_i^{X_L Y_L}(L))). \quad (8)$$

By  $P(X_L, Y_L)$ , we represent the probability of a joint event calculated by  $P(c_i^{X_L(L)Y_L(L)})$ , and by  $P(X_L|Y_L)$ , we represent a conditional probability event representing the probability density of a point falling in the row  $c_i^{Y_L(L)}$  and then being iterated to the column  $c_i^{X_L(L)}$ .

Extended 3-dimensional spaces can be constructed by the composition of  $\Omega^{X_{-L}Y_{-L}}$  with the 1-dimensional space representing the present of variable  $Y$  observed in an order- $L$  partition, or a space constructed from the time-forward trajectory that visits an itinerary of length- $L$  in an order-1 partition. We represent this space by  $(\Omega^{Y_L})$  or  $X(\Omega^{X_L})$ . Notice that a point belonging to a partition in  $c_i^{Y_L}(L)$  will produce an length- $L$  itinerary along the order-1 partition.

We are interested in the spaces  $\Omega^{X_{-L}Y_{-L}Y_L}$  or  $\Omega^{Y_{-L}X_{-L}X_L}$  composed by the variables  $\{X_{-L}(t), Y_{-L}(t), Y_L(t)\}$  or  $\{Y_{-L}(t), X_{-L}(t), X_L(t)\}$ . It will be of further interest the spaces  $\Omega^{Y_{-L}Y_L}$  and  $\Omega^{X_{-L}X_L}$

Figure 2(a) shows the space  $\Omega^{X-LY-LY_L}$  formed by the time-delay coordinates  $X_{-L}$ ,  $Y_{-L}$  and time-forward coordinate  $Y_L$ , with  $L = 1$ , and an order-1 partition in all subspaces defining our probabilistic space. The order-1 partition for the 2D space formed by  $(Y_{-1} \times Y_1)$  shows the symbolic names of columns, rows and the composed cells.

Notice that the 2D space  $\{Y_{-1}, Y_1\}$  with an order-1 partition, where probabilities are calculated (Fig. 2(a)), can be reduced to a 1D space  $W_2^{Y_1Y_{-1}}$  with an order-2 partition (Fig. 2(b)). A partition cell in the space  $W_2^{Y_1Y_{-1}}$  represents point that are in  $c_i^{Y_{-1}}(l)$  and move to  $c_j(1) \in Y_1$ , and therefore produce probabilities of the joint events  $P(Y_{-1}, Y_1) = P(Y_{-1})P(Y_1|Y_{-1})$ . In a general situation, for an arbitrary  $L$ , probabilities in the space  $\{X_{-L}, Y_{-L}\}$  and  $\{Y_{-L}, Y_L\}$  could be calculated over an order- $L$  partition on each subspace. The reduced probabilistic space would be composed by a coordinate  $X_{-L}$  where probabilities are calculated over an order- $L$  partition and the coordinate  $W_{2L}^{Y_{-L}Y_L}$  where probabilities would be calculated over an order- $2L$  partition. A cell in  $W_{2L}^{Y_{-L}Y_L}$  would represent joint events  $P(Y_{-L}, Y_L) = P(Y_{-L})P(Y_L|Y_{-L})$ .

Notice that one can consider subspaces  $X_{-L}$  and  $Y_{-L}$  with an order- $L$  partition each, and the subspace  $Y_J$  with an order- $J$  partition, with  $J \neq L$ , composing the space  $\Omega^{X-LY-LY_J}$ . Then, the reduced space  $W$  would have a probabilistic space formed by a partition of order  $(J+L)$ .

### III. THE TOPOLOGY OF CAUSALITY

#### A. Generating higher-order partitions

We consider two non-coupled Logistic maps ( $\alpha = 0$  in Eq. (1)), represented by  $X$  and  $Y$ , to illustrate how we construct our partitions. Setting  $l_1^X = 0.5$ , if  $x_i \leq l_1^X$  then  $\mathcal{T}(x_i) = 0$  (and  $\mathfrak{s}_i^X(1) = "0"$ ), and if  $x_i > l_1^X$  then  $\mathcal{T}(x_i) = 1$  (and  $\mathfrak{s}_i^X(1) = "1"$ ). Applying these rules for a trajectory of this uncoupled system, we generate Fig. 3(a). In Fig. 3(b), we show in green two columns of the order-2 partition obtained by  $\mathcal{U}^{-1}(l_1^X)$ . Setting  $l_1^Y = 0.5$ , therefore  $\mathcal{L}^{XY} = \{l_1^X, l_1^Y\}$ , we generate Fig. 3(c). The same coloured regions in this figure represent cells in an order-3 partition created by  $\mathcal{U}^{-2}(\mathcal{C}^{XY}(1))$ . The order-3 partition has columns and rows enclosed by straight lines  $\mathcal{L}_X(3) = \mathcal{U}^{-2}(l_1^X(1))$  and  $\mathcal{L}_Y(3) = \mathcal{U}^{-2}(l_1^Y(1))$  respectively, forming the partition  $\mathcal{C}^{XY}(3) = \mathcal{U}^{-2}(\mathcal{C}^{XY}(1))$ . In this case, each column and row have boundaries that describe a generating partition of one Logistic map.

In practice, we do not make pre-iterations of the partition lines to determine the higher-order partitions. Once we choose  $\mathcal{L}_X$  and  $\mathcal{L}_Y$ , the rows, columns, and cells of higher-order partitions are visualised by the colours of points that encode a particular symbolic sequence, using the following algorithm. Given a trajectory, we construct the length- $L$  seg-

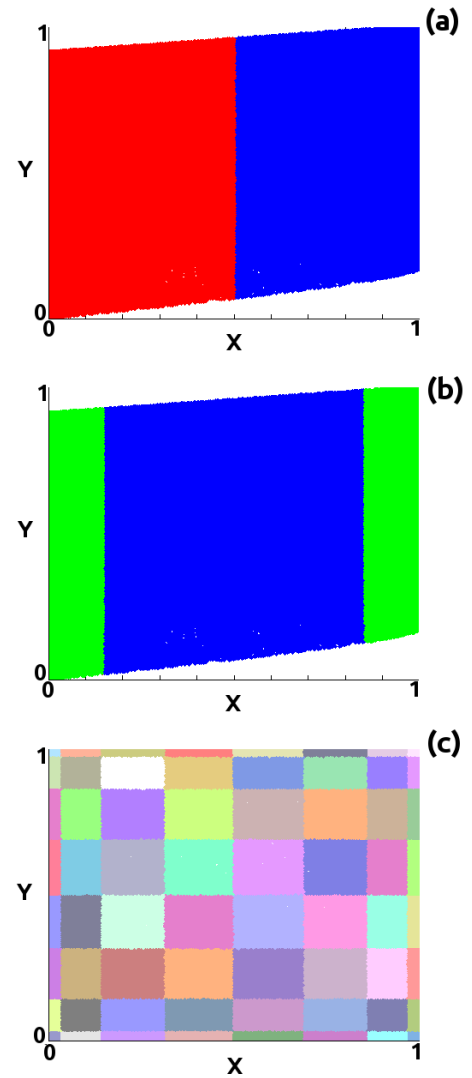


FIG. 3. Panel (a) shows two columns with name  $\mathfrak{s}_1(1) = "0"$  in red and  $\mathfrak{s}_2(1) = "1"$  in blue, for the order-1 partition in  $X$ . Panel (b) shows in green two columns from an order-2 partition in  $X$  with names  $\mathfrak{s}_1(2) = "00"$  and  $\mathfrak{s}_4(2) = "10"$ . Panel (c) shows, by the regions of the same color, cells  $c_i^{XY}(3)$  of an order-3 partition.

ments of it  $\Phi_L^{XY}(n) = \{(x_n^1, x_n^2), \dots, (x_{n+L}^1, x_{n+L}^2)\}$ , and whose symbolic sequence is represented by  $S_L^{XY}(n, 1) = \{\mathfrak{s}_n^X(1), \mathfrak{s}_{n+1}^X(1), \dots, \mathfrak{s}_{n+L-1}^X(1) \bullet \mathfrak{s}_n^Y(1), \mathfrak{s}_{n+1}^Y(1), \dots, \mathfrak{s}_{n+L-1}^Y(1)\}$ . This symbolic sequence is then encoded into an integer number that is used in the palette of colours to set the colour of the point  $(x_n^1, x_n^2)$  that will produce the length- $L$  symbolic sequence  $S_L^{XY}(n, 1)$ . Points will belong to the same column (row) if their symbolic sequence  $S_L^X(n, 1)$  ( $S_L^Y(n, 1)$ ) is the same, and will belong to the same cell if their symbolic sequence  $S_L^{XY}(n, 1)$  is the same. To set the palette of colours, we produce an integer for the colour of the point  $\Phi_L(n) = (x_n^1, x_n^2)$  of an order- $k$  partition generated from an order-1 partition, using the

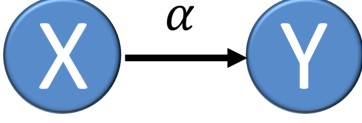


FIG. 4. Two systems directed coupled.

following encoding rule

$$\text{colour}(\Phi_L(n)) = \theta_x(n) * 2^k + \theta_y(n), \quad (9)$$

where  $\theta_x(n) = \sum_{i=1}^L \mathfrak{s}_{n+1-i}^X(1)2^{L-i}$  and  $\theta_y(n) = \sum_{i=1}^{2L} \mathfrak{s}_{n+1-i}^Y(1)2^{2L-i}$ .

### B. Understanding the arrow of influence

We now show how the topological properties of higher-order partitions change according to the coupling strength  $\alpha$  between 2 or more coupled systems as in Eq. (1), and how these topological asymmetries can be used to determine the arrow of influence in these systems.

The symmetry in the structure of the partition in Fig. 3(c) reflects the fact that the two systems are not coupled. Imagine that an observer measure an event in the variable  $Y$  at a time  $n$ :  $Y(n) = x_n^2 = 0.5$ . Applying  $\mathcal{U}^{-k}(l_1^Y)$ , for any  $k$ , will create always a vertical line stretching from 0 to 1, meaning that an observation in  $Y$  at time  $n$  cannot be used to localize the state of the variable  $X$  at time  $n - k$ . The consequence, as we will show next is that there is no flow of information from  $X$  to  $Y$ . The contrary is also true, i.e., one can also use similar arguments to conclude that there is no flow of information from  $Y$  to  $X$ .

For a coupled system represented by Fig. 4, assuming a coupling strength of  $\alpha = 0.09$ , we have created partitions of different orders (from order-1 to order-5) and shown in Fig. 5. One can see how the increase of the order increases the topological complexity of the partitions, for example going from Fig. 5(a) to Fig. 5(d). Paying attention to the higher order rows, defined by the enclosure of  $\mathcal{U}^{-k}(l_1^Y)$  along the  $Y$  variable, in Fig. 5(e-h), and the higher-order columns, defined by enclosure of  $\mathcal{U}^{-k}(l_1^X)$ , we can observe how they are not enclosed any longer by straight lines. This asymmetry is the consequence of  $X$  driving  $Y$ .

We now want to analyse the different topological features of the higher-order partitions when we consider different orders in  $X$  and  $Y$ . For that we produce Fig. 6 obtained from two directed-coupled Logistic maps as showed in Fig. 4 with a coupling strength  $\alpha = 0.09$ . We have selected two orders for our partitions in  $X$  and  $Y$ : 2

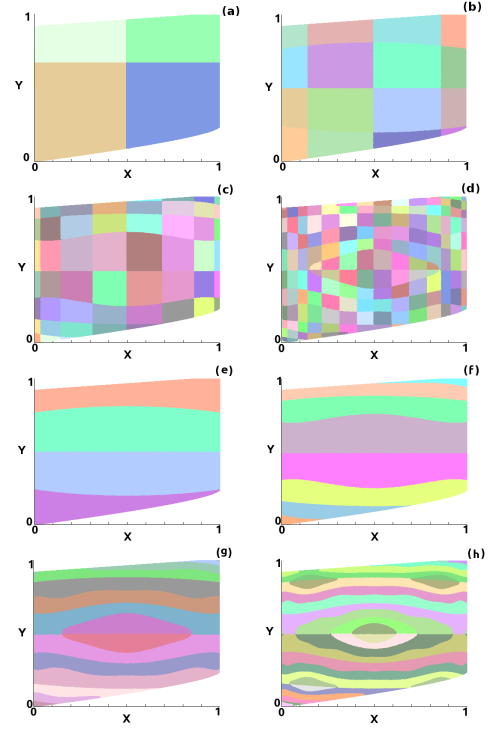


FIG. 5. Panel (a) shows an order-1 partition  $\mathcal{C}_1^{XY}$ , each coloured region represents a cell. Panel (b) shows the order-2 partition given by  $\mathcal{C}_1^{XY} = \mathcal{U}^{-1}(\mathcal{C}^{XY}(1))$ . Panels (c-d) show the corresponding order-3 and order-4 partitions, generated by  $\mathcal{U}^{-2}(\mathcal{C}^{XY}(1))$  and  $\mathcal{U}^{-3}(\mathcal{C}^{XY}(1))$  respectively, coloured regions represent the cells in the partition. Panels (e-g) show  $\mathcal{U}^{-1}(l^Y(1))$ ,  $\mathcal{U}^{-2}(l^Y(1))$  and  $\mathcal{U}^{-3}(l^Y(1))$  respectively, and each coloured "horizontal" stripe represents a higher-order row. Finally panel (h) shows only the higher-order rows of an order-5 partition, enclosed by  $\mathcal{U}^{-4}(l^Y(1))$ .

and 5. Figure 6 (a) shows the different cells (same colour region) of a partition created by the intersection of an order 2 partition in  $X$  and order 5 partition in  $Y$ . Figure 6(b) shows the different cells of a partition of an order 2 in  $Y$  and an order 5 in  $X$ . The asymmetry in Fig. 6(a) indicates that the system has an arrow of influence  $X \rightarrow Y$ .

### C. Local mutual information

Pointwise mutual information (PMI) is a probabilistic measure of the amount of information that two different random variables possess locally between them. Given a particular partition, the PMI only takes into consideration the information computed over a single cell and not over the entire set of cells as the MI. PMI is defined as

$$PMI(i, j) = H_X^i + H_Y^j - H_{XY}^{i,j}, \quad (10)$$

where:  $H_X^i = -P(\mathfrak{s}_i^X) \log(P(\mathfrak{s}_i^X))$ ,  $H_Y^j = -P(\mathfrak{s}_j^Y) \log(P(\mathfrak{s}_j^Y))$ , and  $H_{XY}^{i,j} = -P(\mathfrak{s}_k^{XY}) \log(P(\mathfrak{s}_k^{XY}))$ ,

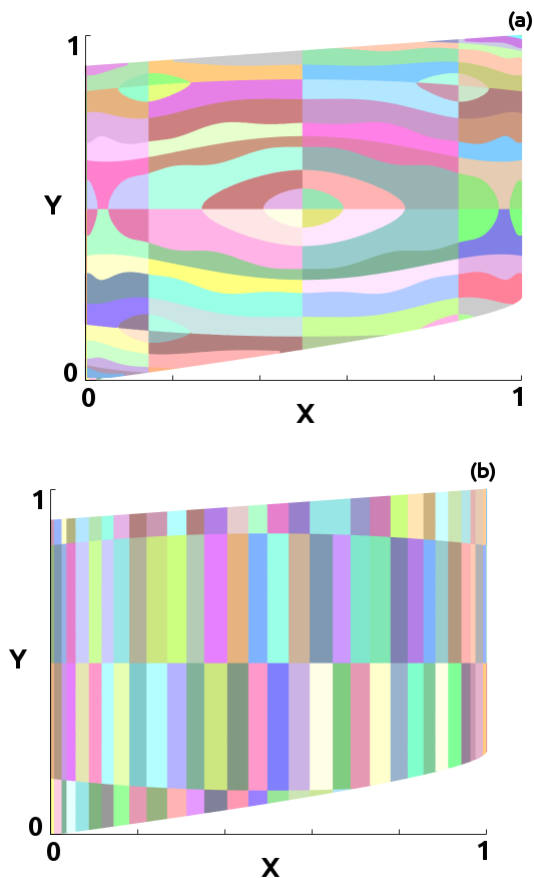


FIG. 6. Panel (a) shows the partition of order 5 in  $Y$  and order 2 in  $X$ . Panel (b) shows the partition of order 2 in  $Y$  and order 5 in  $X$ .

with  $k$  representing the cell formed by the overlapping of the higher-order row  $i$  with the higher-order column  $j$ . Therefore, MI is just the average of PMI over cells of the partition. In the following, we consider a normalized variant of PMI, named normalized Pointwise Mutual Information (nPMI), introduced in Ref.<sup>24</sup>, and defined as:

$$nPMI = \frac{PMI(i, j)}{\log(P(\mathfrak{s}_k^{XY}))}. \quad (11)$$

The advantage of the nPMI over PMI is the reduction of the sensitivity of the measure to short time-series.

Using nPMI in the partitions considered in Fig. 6, we can calculate the amount of information exchanged between variables  $X$  and  $Y$ , when they are being encoded by symbolic sequences of different lengths. As we shall see in the next section, this quantity actually can be used to infer the directionality of the flow of information being transferred.

Figure 7 shows the nPMI for two directed coupled Logistic maps for an order-5 partition  $\mathcal{C}^{XY}$  as the order of the partition along the variable  $Y$  in Fig. 6(a). The

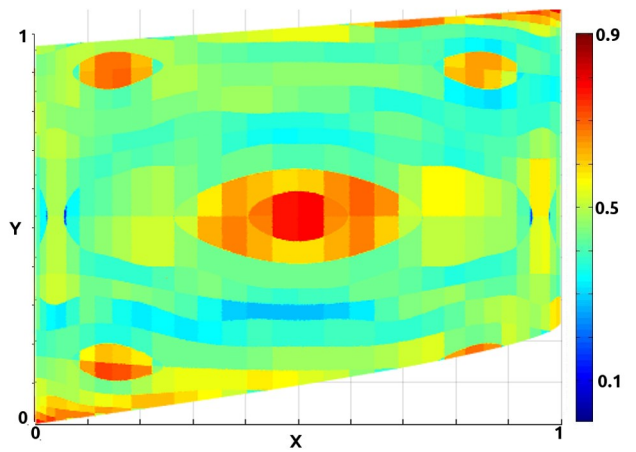


FIG. 7. nPMI for a directed coupled Logistic map with a coupling strength of 0.09. It can be observed how the nPMI is higher inside the bubbles.

surprising fact is that nPMI is larger for a special union of cells enclosed by one of the solutions of  $\mathcal{U}^{-3}(l_1^Y)$  that forms closed curves. We call these special union of cells, causal bubbles, from its closed graphical representation. We can see that the bubbles are areas containing trajectory points responsible for a large amount of information exchanged between  $X$  and  $Y$ , and as explained in the following, a consequence of the fact that  $X \rightarrow Y$ .

#### D. Causal bubbles

Figure 8 shows an illustration of how these bubbles are created. The partition line  $l_1^Y$  represented by the black dashed line in panel (a) is iterated once producing the red curves such as the ones showed in panel (b), and eventually after  $2L - 1$  backwards iterations these curves form a closed contour as is shown in panel (c) by the closed red curves.

Assume that the future of the observed variable  $y_{t+L-1}$ ,  $L$  iterations forward in  $y$ , has a value that lays exactly at the partition line, i.e.  $y_{t+L-1} \in l_1^Y$ . The variable to be predicted has an arbitrary value at  $t+L-1$ , so  $x_{t+L-1}$  can assume any value in the state space. Then, after one backward iteration,  $y_{t+L-2} \in \mathcal{U}^{-1}(l_1^Y)$  is located on the red lines in panel (b). After  $2L-1$  backward iterations  $y_{t-L}$  has a position along the red closed curve in panel (c), enclosing a bubble area.

Therefore, the first observation in the variable  $y$  at time  $t + L - 1$  cannot tell anything about the position of the variable  $x_{t+L-1}$ . Assuming the observer has full knowledge of the dynamical equations, it makes one observation at  $y$  obtaining the value  $y_{t+L-1}$ , which in this imaginary example lays at  $l_1^Y$ . The smart observer uses the knowledge of the dynamics and makes  $2L - 1$  backward iteration of  $l_1^Y$ . The observer will conclude that, if  $y_{t+L-1} \in l_1^Y$ , then  $y_{t-L} \in I_Y$  and  $x_{t-L} \in I_X$ , where  $I_X$  is

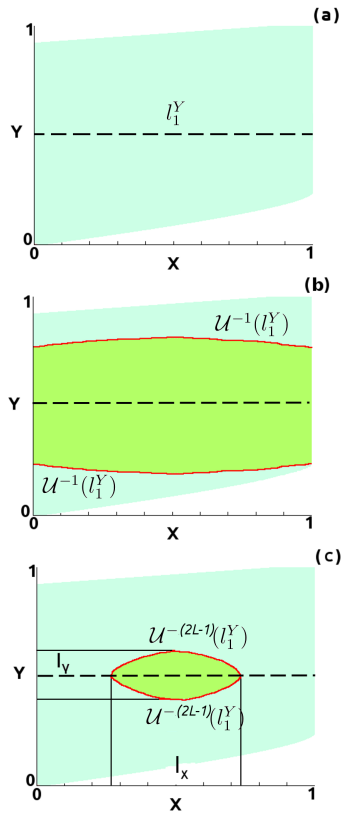


FIG. 8. (a) Dashed black line represents  $l_1^Y$ . (b) The red curves are obtained by one backward iteration of  $l_1^Y$ . (c) The closed red curve is obtained by  $2L - 1$  backward iterations of  $l_1^Y$ .

the  $x$ -interval enclosed by the red curve, panel(c). So, by making one observation of the future of  $y$  and using the knowledge of the dynamics (which can be obtained by modelling the system), the observer can better localize the state of the past variable  $x$ , if  $X \rightarrow Y$ . Moreover, if more observations are done (from the future to the past) in  $y$ , more likely the observer is to improve its knowledge about the location of  $x_{t-L}$  by doing similar analysis.

If there is no physical connection between system  $X$  and system  $Y$ , and no flow of information from  $X$  to  $Y$ , the bubbles are not formed, and therefore, one cannot localize the position of the variable  $X$  by observing  $Y$ .

#### IV. CAUSAL MUTUAL INFORMATION (CAMI)

We are now ready to define a new informational quantity named *Causal Mutual Information* from  $X$  to  $Y$  ( $\text{CaMI}_{X \rightarrow Y}$ ) as the mutual information between joint events in  $X_{-L}$  and the set composed by the joint events of  $Y_{-L}$  and  $Y_L$  as

$$\text{CaMI}_{X \rightarrow Y} = MI(X_{-L}; (Y_{-L}, Y_L)) = MI(X_{-L}; W_{2L}^{Y_L Y_{-L}}). \quad (12)$$

Analogously,  $\text{CaMI}_{Y \rightarrow X} = MI(Y_{-L}; W_{2L}^{X_L X_{-L}})$ .

Notice that  $\text{CaMI}$  is not permutable since,  $\text{CaMI}_{X \rightarrow Y} \neq \text{CaMI}_{Y \rightarrow X}$ . As we can see,  $\text{CaMI}_{X \rightarrow Y}$  is the Mutual information between trajectory points in the subspace  $X_L$  and the subspace  $W_{2L}^{Y_L Y_{-L}}$  and that measures the amount of information between longer time-series of past, present and future of  $Y$  and shorter time-series of the past of  $X$ . The fundamental idea behind the reason for us to propose  $\text{CaMI}$  as a measure of causality is that if there is a flow of information from  $X$  to  $Y$ , then longer observations in the  $Y$  variable can be used to predict the past of states of  $X$ .  $\text{CaMI}$  is also a quantity that measures the total amount of information extracted from one variable by observing another variable, not only the shared amount (non causal) but also the transmitted amount (causal).

Considering the coupled system and the same partition used to create Fig. 6(a), the magnitude of the computed  $\text{CaMI}_{X \rightarrow Y}$  is 0.17. Considering the coupled system and the same partition used to create Fig. 6(b), the magnitude of the computed  $\text{CaMI}_{Y \rightarrow X}$  is 0.04. The difference in the  $\text{CaMI}$ 's magnitudes, meaning  $\text{CaMI}_{X \rightarrow Y} - \text{CaMI}_{Y \rightarrow X} > 0$ , and the asymmetry in Fig. 6(a) with the existence of the causal bubbles indicate the presence of a system whose direction of causality is given by  $X \rightarrow Y$ , and therefore, there is a flow of influence from  $X$  to  $Y$ .

Notice that the PMI as defined in Eq. (10) is just one of the terms considered in the calculation of  $\text{CaMI}$ .

#### A. Transfer Entropy and Causal Mutual Information

Having two random processes  $X$  and  $Y$ , the amount of information transferred from process  $X$  to  $Y$  ( $X \rightarrow Y$ ) can be quantified by the Transfer Entropy<sup>5</sup>, defined as:

$$T_{X \rightarrow Y} = H(Y_L | Y_{-L}) - H(Y_L | Y_{-L}, X_{-L}), \quad (13)$$

where  $H(X)$  is the Shannon's entropy of  $X$ ,  $H(X_L | Y_{-L})$  is the knowledge (reduce of entropy) of process  $X$  from time  $t$  to  $t + L - 1$  if the past of process  $Y$  from  $t - 1$  to  $t - L$  is known, and  $H(Y_L | Y_{-L}, X_{-L})$  represents the knowledge of the process  $Y$  from time  $t$  to  $t + L - 1$ , if the past of  $X$  and  $Y$  in the interval from  $t - 1$  to  $t - L$  is known. Transfer entropy was shown to be related to another famous causality measure<sup>25,26</sup>, the directed information, directed information being a cumulative version of transfer entropy, and being currently considered the appropriated measure to deal with channels of communication with feed-back, those where the output is feed-backed to the input of the channel.

We can express Eq. (13) as a function of joint entropies and not conditional one using Bayes theorem:

$$T_{X \rightarrow Y} = H(Y_{-L}, Y_L) + H(Y_{-L}, X_{-L}) - H(Y_{-L}) - H(Y_{-L}, X_{-L}, Y_L). \quad (14)$$

Using the equality  $MI(X, (Y, Z)) = H(X) + H(Y, Z) -$

$H(X, Y, Z)$ , we have,

$$T_{X \rightarrow Y} = H(Y_{-L}, Y_L) + H(Y_{-L}, X_{-L}) - H(Y_{-L}) - H(Y_{-L}, Y_L) - H(X_{-L}) + MI(X_{-L}, (Y_{-L}, Y_L)). \quad (15)$$

Finally using Eq. (12), we conclude that

$$CaMI_{X \rightarrow Y} = T_{X \rightarrow Y} + MI(X_{-L}; Y_{-L}), \quad (16)$$

where  $MI(X_{-L}; Y_{-L}) = H(Y_{-L}) + H(X_{-L}) - H(Y_{-L}, X_{-L})$  is the mutual information of the system composed by  $X$  and  $Y$ . Both quantities are shown over a Venn diagram in Fig. 9 for their comparison. One can see that CaMI carries more information about the considered variables than transfer entropy.  $CaMI_{X \rightarrow Y}$  represents the amount of information exchanged between  $X$  and  $Y$  (provided by the term  $MI(X_{-L}; Y_{-L})$ ) and the transfer entropy from  $X$  to  $Y$ . Whereas  $MI(X_{-L}; Y_{-L})$  measures how much the observation of a length- $L$  trajectory along the variable  $X$  (or  $Y$ ) can be predicted by observations of a length- $L$  trajectory of the variable  $Y$  (or  $X$ ), the transfer entropy from  $X$  to  $Y$  measures how much one can predict from the past state of the  $X$  by making observations of the past, present, and future states of the variable  $Y$ .

One important fact to notice is that since  $MI(X_{-L}; Y_{-L}) = MI(Y_{-L}; X_{-L})$ , the directionality index defined by  $T_{X \rightarrow Y} - T_{Y \rightarrow X}$ , and therefore representing the net flow of information between both variables, can be calculated by

$$DI = T_{X \rightarrow Y} - T_{Y \rightarrow X} = CaMI_{X \rightarrow Y} - CaMI_{Y \rightarrow X}. \quad (17)$$

As another remark, notice that transfer entropy is defined as the conditional mutual information and therefore,  $T(X \rightarrow Y) = MI(X_{-L}; Y_L | Y_{-L})$ , see Ref.<sup>6</sup>. Recalling that  $CaMI_{X \rightarrow Y} = MI(X_{-L}; (Y_{-L}, Y_L))$ , it is easy to see that to define CaMI we have replaced the conditional probabilities in the transfer entropy  $T_{X \rightarrow Y}$  to joint probability ones in  $CaMI_{X \rightarrow Y}$ .

## V. HIGHER-ORDER MARGINAL PARTITIONS

We have previously seen that a higher-order 2D asymmetric partition, where each coordinate has different orders, can be used to calculate CaMI. This higher-order partition is expected to be generating and unique, so that Eqs. (5) and (7) can be used instead of Eqs. (6) and (8). If the initial marginal order- $m$  partition is used to generate the higher order partitions, observations need to be taken considering a resolution provided by the order- $m$  partition. In a general situation, or when dealing with a stochastic dynamics, we should not expect that higher-order generating partitions are unique. It is thus interesting to verify whether a marginal partition of order  $m$  along the variable  $X$  ( $\mathcal{L}_X(m)$ ) and a marginal partition of order  $2m$  along the variable  $Y$  ( $\mathcal{L}_Y(2m)$ ) could

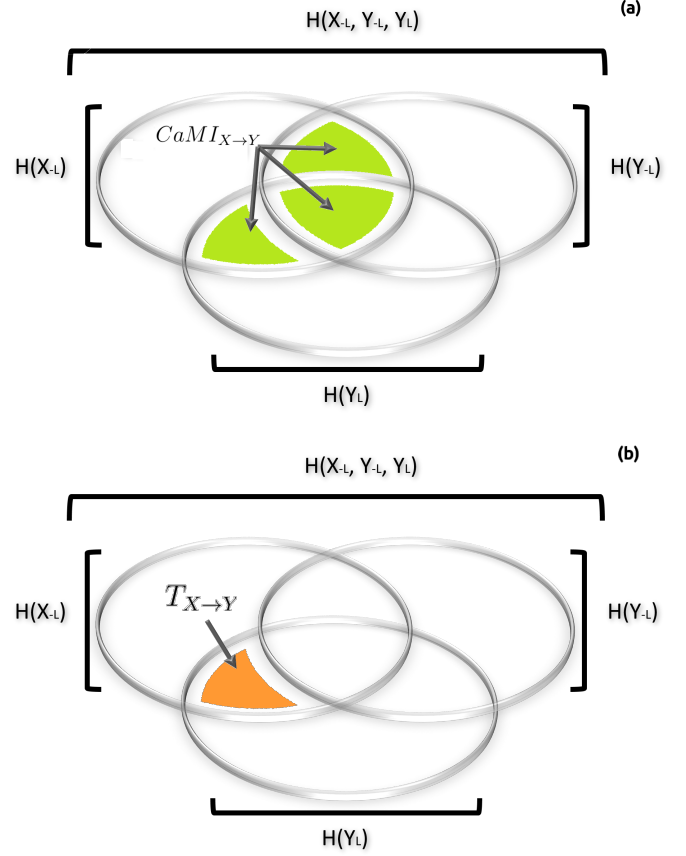


FIG. 9. Representation over a Venn diagram of the CaMI. Panel (a): Causal Mutual Information,  $CaMI_{X \rightarrow Y}$ . Panel (b): Transfer entropy,  $T_{X \rightarrow Y}$ .

be used to calculate  $CaMI_{X \rightarrow Y}$ .  $CaMI$  calculated in this way would be measuring the mutual information between lower-resolution observation along the variable  $X$  and higher-resolutions observations along the variable  $Y$ .

To show that this can be indeed done, we analyse the mutual information of a system (as the one shown in Fig. 10), with a coupling strength  $\alpha = \{0, 0.05, 0.1\}$  and  $\beta = 0.1 - \alpha$ . In Fig. 11, we show by colors the values of the MI calculated considering Eqs. (5) and (7) between variables  $X$  and  $Y$  for a partition  $\mathcal{C}^X$  for  $X$  and  $\mathcal{C}^Y$  for  $Y$ , with different number of columns and rows, respectively. The number of  $N_X$  and  $N_Y$  are shown in the axis of Fig. 11. Recall that  $CaMI_{X \rightarrow Y}$  is just the mutual information between variables  $X$  and  $Y$  where the partition of  $X$  has order  $L$  and the partition of  $Y$  has order  $2L$ . We, therefore, want to test whether only MI is capable of detecting the direction for the flow of information when a higher-order probabilistic space that has arbitrary equal rectangular areas are considered.

In Figs 11(a)-(c), if the partition in  $X$  has the same number of cells than the partition in  $Y$ , MI grows with the growing of the number of cells. As expected, one can see that if the flow of information is from  $X \rightarrow Y$  (as in

panel (a)), then partitions with more cells in  $Y$  than in  $X$  produce larger MI (or CaMI) than partition with less cells in  $Y$  than in  $X$ .

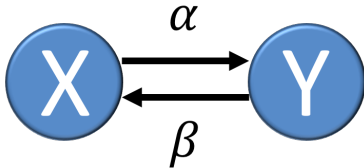


FIG. 10. Two Logistic maps bi-directionally coupled. The coupling strengths  $\alpha$  and  $\beta$  are related by  $\beta = 0.1 - \alpha$ .

Surprisingly, Fig. 11(a) shows a novel feature for the MI of coupled systems. If the flow of information goes from  $X \rightarrow Y$ , then given a partition in  $Y$  with a particular number of cells (i.e., resolution), the value of MI obtained is roughly invariant for the chosen resolution in  $X$ . This implies that the amount of information one can realize from  $X$  by making measurements in  $Y$  is almost solely dependent on the resolution of the observation, if the flow of information goes from  $X$  to  $Y$  and there is a sufficient large amount of number of cells in  $Y$ . In Fig. 11(b) the flow of information goes from  $Y$  to  $X$  and therefore, for a sufficiently large number of cells in  $X$ , the information that one can deduce from  $Y$  by measuring  $X$  almost solely depends on the resolution of  $X$ . Finally, in Fig. 11(c) for the bidirectionally coupled system, with equal coupling strengths, one has that the values for MI will depend on both resolution of variables  $X$  and  $Y$  in a complementary way, i.e. if the sum of the number of rows and columns is maintained, MI remains roughly invariant. In fact the relationship is described by a diagonal hyperbola.

We conclude that an important variable to study in a system is the dependant driven variable. Measuring this variable with finer resolution allows us to obtain more information about the driving system.

## VI. CONCLUSION

In this work, we have investigated the space-time properties of causality, causality meaning the study of the arrow of influence between two systems.  $X$  is said to cause an effect in  $Y$ , if the predictability (uncertainty) about the future states of  $Y$  increases (decreases) as its own past and the past of  $X$  are taken into consideration. We have shown that this notion of causality leads to a more natural, unifying, and simple definition for it: to detect whether a system  $X$  causes an effect in system  $Y$ , observations of past and future events in only the variable  $Y$  is sufficient to predict past states of  $X$ , or to reduce the uncertainty about the past state of  $X$ . This fundamental time property of causality will lead to a fundamental spatial property of causality. To detect a flow of

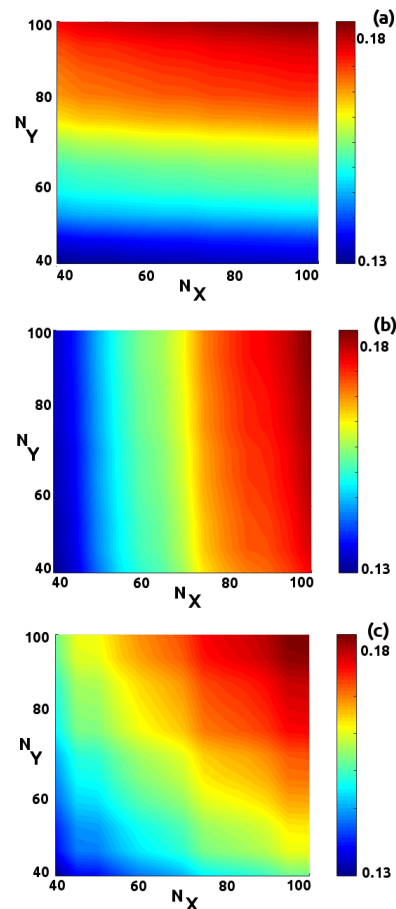


FIG. 11. Mutual information of coupled Logistic maps computed on an asymmetric partition with different number of rows and columns. The horizontal and vertical axis show the different amount of rows and columns of the partition. Panel (a) shows the result for  $\alpha = 0$  and  $\beta = 0.1$ . Panel (b) the results for  $\alpha = 0.1$  and  $\beta = 0$ . Panel(c) shows the result for  $\alpha = 0.05$  and  $\beta = 0.05$

influence from  $X$  to  $Y$ , either one can measure the symmetric quantity mutual information between shorter time-series of  $X$  and longer time-series of  $Y$ , an approach that explores the time nature of causality, or one can calculate the mutual information between lower precision measured time-series in  $X$  and higher precision measured time-series in  $Y$ , an approach that explores the space nature of causality. Causality can be detected not only by the analyses of the topological properties of higher-order partitions generated by lower-order marginal partitions (the "space" property of causality), but also by considering the probabilities on these partitions, reflecting the density of trajectories of a given time-length (the "time" property of causality).

To apply this abstract notion of causality into a quantitative approach, we have introduced a new informational quantity, the causal mutual information,  $\text{CaMI}_{X \rightarrow Y}$  that measures the total amount of information being transmitted from  $X$  to  $Y$ , the information shared between both

variables and that can be used to predict the present state of  $X$  by observations in  $Y$ , and the information directed transmitted from  $X$  to  $Y$ , which can be used to predict the past states of  $X$  by observations of the past and future states of  $Y$ .

Since CaMI does not require the calculations of conditional probabilities, but rather only joint probabilities, the probabilistic spaces involved in its calculation can be lower-dimensional, enabling a quick calculation of it, this offering a causality study with less computational efforts. This property of CaMI could be advantageously used to create a practical brain-based cryptography (see Ref.<sup>27</sup>), which requires the quick calculation of causality measures. Also, less data is required for the determination of causality, since the probability space can be constructed according to the available data.

- <sup>1</sup>J. M. Mooij, D. Janzing, and B. Schölkopf, in *NIPS Causality: Objectives and Assessment* (2010) pp. 147–156.
- <sup>2</sup>I. Guyon, D. Janzing, and B. Schölkopf, (2012).
- <sup>3</sup>Y. Kano and S. Shimizu, in *Proceedings of the International Symposium on Science of Modeling, the 30th Anniversary of the Information Criterion* (2003) pp. 261–270.
- <sup>4</sup>C. W. Granger, *Econometrica: Journal of the Econometric Society*, 424 (1969).
- <sup>5</sup>T. Schreiber, *Physical review letters* **85**, 461 (2000).
- <sup>6</sup>M. Paluš, *Physica D: Nonlinear Phenomena* **93**, 64 (1996).
- <sup>7</sup>Y. Hirata and K. Aihara, *Physical Review E* **81**, 016203 (2010).
- <sup>8</sup>S. Haufe, V. V. Nikulin, K.-R. Müller, and G. Nolte, *NeuroImage* **64**, 120 (2013).
- <sup>9</sup>Y. Chen, G. Rangarajan, J. Feng, and M. Ding, *Physics Letters A* **324**, 26 (2004).
- <sup>10</sup>N. Ancona, D. Marinazzo, and S. Stramaglia, *Physical Review E* **70**, 056221 (2004).
- <sup>11</sup>E. Bollt, P. Gora, A. Ostruszka, and K. Zyczkowski, *SIAM Journal on Applied Dynamical Systems* **7**, 341 (2008).
- <sup>12</sup>C. W. Granger, *Journal of Economic Dynamics and control* **2**, 329 (1980).
- <sup>13</sup>C. W. Granger, *Journal of econometrics* **39**, 199 (1988).
- <sup>14</sup>P.-O. Amblard and O. J. Michel, *Journal of computational neuroscience* **30**, 7 (2011).
- <sup>15</sup>M. Takigawa, G. Wang, H. Kawasaki, and H. Fukuzako, *International journal of psychophysiology* **21**, 65 (1996).
- <sup>16</sup>L. A. Baccalá and K. Sameshima, *Biological cybernetics* **84**, 463 (2001).
- <sup>17</sup>M. Kaminski and K. J. Blinowska, *Biological cybernetics* **65**, 203 (1991).
- <sup>18</sup>H. Marko, *IEEE Transactions on communications* **21**, 1345 (1973).
- <sup>19</sup>V. A. Vakorin, O. A. Krakovska, and A. R. McIntosh, *Journal of neuroscience methods* **184**, 152 (2009).
- <sup>20</sup>I. Vlachos and D. Kugiumtzis, *Physical Review E* **82**, 016207 (2010).
- <sup>21</sup>J. Runge, *Physical Review E* **92**, 062829 (2015).
- <sup>22</sup>S. Mangiarotti, *Chaos, Solitons & Fractals* **81**, 184 (2015).
- <sup>23</sup>P. Myrberg, *J. Math. Pures Appl.*(9) **41**, 339 (1962).
- <sup>24</sup>G. Bouma, *Proceedings of GSCL*, 31 (2009).
- <sup>25</sup>N. J. Newton, arXiv preprint arXiv:1604.01969 (2016).
- <sup>26</sup>Y. Liu and S. Aviyente, in *2012 IEEE Statistical Signal Processing Workshop (SSP)* (IEEE, 2012) pp. 73–76.
- <sup>27</sup>R. Szmoski, F. Ferrari, S. d. S. Pinto, M. Baptista, and R. Viana, *Physics Letters A* **377**, 760 (2013).